SCIENTIFIC REPORTS
natureresearch

OPEN

Catalytic oxidation of toluene, ethyl acetate and chlorobenzene over Ag/MnO$_2$-cordierite molded catalyst

Jianan Zhu[1], Wenrui Zhang[1], Qiuping Qi[1], Huawei Zhang[1], Yaqing Zhang[1], Dekui Sun[2] & Peng Liang[1]

Multi-structured Ag/MnO$_2$-cordierite molded catalysts were prepared by hydrothermal method and applied to the catalytic oxidation of VOCs. Catalytic activities of Ag/MnO$_2$-cordierite were evaluated by 1000 ppm of toluene, ethyl acetate and chlorobenzene degradation respectively at the air atmosphere, and their physicochemical properties were characterized through multiple techniques containing XRD, SEM, TEM, H$_2$-TPR and XPS. It is found that nanorod Ag/MnO$_2$-cordierite molded catalyst showed prominent catalytic activity for VOCs decomposition and the T$_{90}$ for toluene, ethyl acetate and chlorobenzene are 275 °C, 217 °C and 385 °C respectively under the space velocity of 10,000 h^{-1}. High valence manganese oxide, more active lattice oxygen proportion and superior low-temperature reducibility were the great contributors to the high activity of the catalyst with nanorod morphology. Studies of space velocity and catalytic stability over nanorod Ag/MnO$_2$-cordierite molded catalyst have confirmed the good catalytic performance, excellent mechanical strength and satisfied anti-toxicity to Cl at higher space velocity, which indicates that this molded catalyst have promise for industrial application.

Volatile organic compounds (VOCs) are classified as an indispensable cause for the current atmospheric pollution[1,2]. Due to the high chemical stability, toxicity and carcinogenic effect, VOCs pose serious threats to human health and ecological environment[3,4]. However, the growing emissions of VOCs owing to rapid urbanization and industrialization make it urgent to control and removal VOCs effectively[5]. Among the numerous approaches, catalytic oxidation is widely recognized as an effective and broad technique to degrade the industrial VOCs due to its low energy consumption, high purification efficiency, heat recovery and so on[6,7]. Therefore, the study of low-temperature, high-activity and anti-poisoning catalysts is a key to the catalytic oxidation in industrial process.

Many catalysts can be used for catalytic oxidation of VOCs[8–12]. Recent studies showed supported transition metal oxides catalysts such as VO$_x$, MnO$_x$ and WO$_x$ have been applied widely and efficiently[8–10]. Specially, manganese dioxides have attracted extensive attentions because of its high selectivity and activity at low temperature[11–13]. However, some drawbacks such as poor stability, sintering and low conversion rate prevent more general applications. Articles reported presently that the incorporation of noble metals, such as Pt, Au and Ag, can promote the oxidation of VOCs and enhance the anti-toxicity of the catalyst effectively because of their higher activity for the break of C-C bond, C-H bond and C-Cl bond[14–17]. For example, the Au/Mn$_2$O$_3$ powdered catalyst prepared by Xie et al.[15] achieved 90% conversion of toluene at the conditions of volume ratio of toluene to O$_2$ of 1:400, 258 °C and space velocity of 40,000 ml/(g·h). Xia et al.[18] prepared the nanotube Au-Pd/α-MnO$_2$ powdered catalyst and observed the good catalytic activity for VOCs oxidation with 40–60 mesh quartz sand in a quartz tube with an inner diameter of 4 mm. The studies reported[7,12,18–20] so far are mostly carried out by mixing the pure powdered catalyst into the millimeter-scale quartz tube reactor through incorporating inert material such as quartz sand. However, they are unsuitable for actual catalytic combustion owing to incomplete reaction between

[1]College of Chemical and Environmental Engineering, Shandong University of Science and Technology, Qingdao, Shandong, 266590, P.R. China. [2]State Key Laboratory of Coal Conversion, Institute of Coal Chemistry, Chinese Academy of Sciences, Taiyuan, Shanxi, 030001, P.R. China. Correspondence and requests for materials should be addressed to W.Z. (email: wenrui.mao@163.com) or P.L. (email: liangpeng202@hotmail.com)
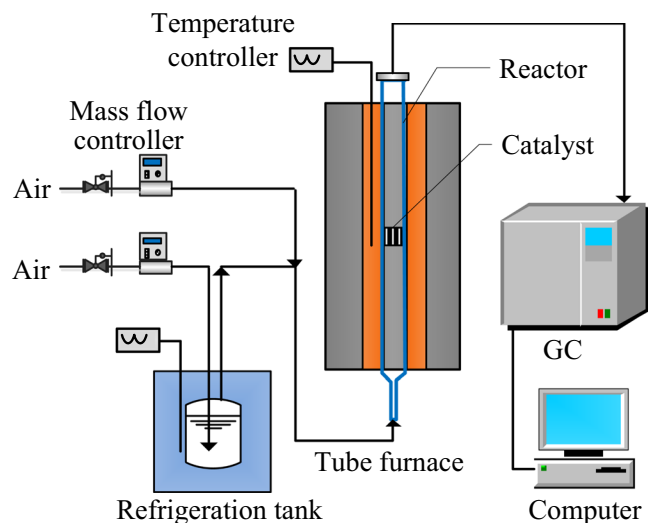
Figure 1. Schematic diagram of catalysts evaluation device.

catalyst and reactants under high volume space velocity, and most of them were applied to degrade one kind of VOCs in the atmosphere with high oxygen content. There are few researches about lower temperature catalytic degradation of various VOCs and chlorinated volatile organic compound (Cl-VOCs) in actual industrial exhaust gas treatment. Moreover, catalysts which can completely destroy Cl-VOCs are restricted by high temperatures and serious deactivation in the presence of Cl[21–23]. Studies[24] have shown that the molded catalyst can offer lower mass transfer resistance and higher diffusion efficiency, which can be a promoter for excellent catalytic activity for VOCs degradation. Cordierite[25,26] has been widely used as carrier because of its superior mechanical stability and hydrothermal stability as well as its plasticity. For example, Mn-Co-Ce/cordierite catalyst[27] and Cr-MnO$_2$/cordierite catalyst[28] increased the external mass transfer rate to optimize the catalytic combustion performance of Cl-VOCs. In previous work[20], Ag/MnO$_2$ powdered catalyst was prepared to degrade toluene. It has observed that excellent catalytic oxidation performance due to the multiple valence state of Mn and the better oxygen transformation between transition metal oxides in the redox reaction by Ag. Therefore, Ag/MnO$_2$ may be a promising catalytic oxidation of VOCs. However, there are few studies of cordierite coated by Ag/MnO$_2$ molded catalyst.

In this work, the Ag/MnO$_2$ catalysts with different morphology supported on cordierite were synthesized through a liquid phase reduction method and then were used for catalytic degradation of toluene, ethyl acetate and chlorobenzene. Additionally, combined with the activity and physical property characterization results of the catalyst, the structure-activity relationship of the catalyst and the cause of the chlorine poisoning of the catalyst were investigated.

Methods

Catalysts preparation. The nanorod MnO$_2$ and nanotube MnO$_2$ were synthesized by hydrothermal method published in previous papers[12,20], and the preparation details of the MnO$_2$ precursors were described in SI-1. The Ag/MnO$_2$ catalyst was synthesized by a liquid phase reduction method. Typically, quantitative MnO$_2$ powder was firstly dispersed in 0.01 mol/l AgNO$_3$ (in accordance with the silver loading of 2 wt%) and stirred for 2 h at room temperature to obtain a homogenous suspension. The desired volume NaBH$_4$ aqueous solution (theoretical molar ratio of NaBH$_4$: Ag$^+$ = 2:1) was added to the suspension, followed by stirring until the reaction was finished. Next, the products were filtered, washed by deionized water and then dried at 80 °C. According to their results of morphology, the names of samples were donated as the R-Ag/MnO$_2$ (nanorod Ag/MnO$_2$) and T-Ag/MnO$_2$ (nanotube Ag/MnO$_2$). Finally, the Ag/MnO$_2$ catalysts supported on cordierite (the diameter of 2 cm and height of 1 cm, 200 mesh) were manufactured using a wet impregnation method with aluminum sol as a binder. The samples were subsequently dried in an oven of 100 °C for 1 h and then calcined in a muffle furnace at 300 °C for 3 h.

Catalytic activity tests. Catalytic activity was implemented by a self-assembled tubular fixed bed reactor within the temperature range 80–450 °C (Fig. 1). The flow rates of each gas path were calculated based on the saturated vapor pressure of VOCs and controlled by the mass flow meters. The bubbling gas stream passed through the liquid organic matter and then merged with the equilibrium gas to obtain the desired concentration of VOCs gas, which then entered the tube furnace and reacted with the catalysts in the middle of the quartz tube. The concentration of VOCs before and after the reaction at different temperatures was obtained using the on-line gas chromatograph (GC-9790) outfitted with a flame ionization detector (FID) and a capillary column (ONLYSCI, China) of 50 m * 0.32 mm * 0.5 μm. By the way, the products of three VOCs have been identified as CO$_2$ and H$_2$O by clarify lime water and anhydrous copper sulfate, where HCl appeared in the oxidation products of chlorobenzene by detection of a silver nitrate solution. Meanwhile, the blank test was performed without catalysts to ensure the accuracy and reliability of experiments.

The VOCs conversion was calculated according to the following equation, where C$_{In}$ and C$_{Out}$ represented the concentration of VOCs in the gas before and after the reaction, respectively.
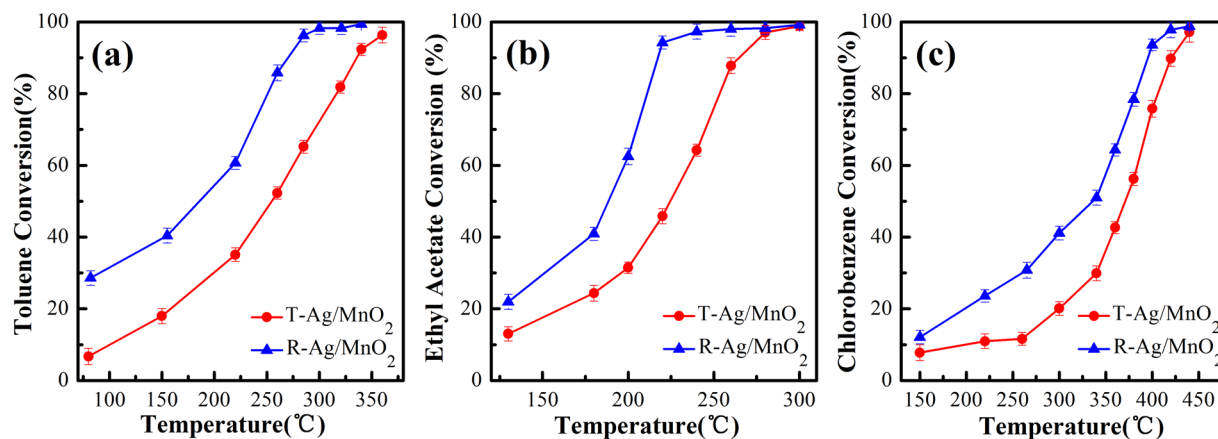
Figure 2. Catalytic activity of Ag/MnO$_2$-cordierite catalyst for (**a**) toluene, (**b**) ethyl acetate, (**c**) chlorobenzene at different temperatures; reaction conditions: VOCs = 1000 ppm; catalyst content = 0.1 g/cm^3; SV (space velocity) = 10,000 h^{-1}.

$$Conversion = (1 - C_{Out}/C_{In}) \times 100\% \qquad (1)$$

Characterization of catalysts. The elemental compositions of the catalysts were measured using an Agilent 7500cx inductively coupled plasma spectrometry (ICP). The morphology of the catalysts was obtained by scanning electron microscopy (SEM, model numbers was JEOL, JSM-7800F) operating at 10 kV after precoating the samples with gold (ion sputtering apparatus, JFC1600) and transmission electron microscopy (TEM, model numbers was FEI Tecnai G2 F20) at an accelerating voltage of 200Kv. X-ray diffraction (XRD) patterns were performed by a Rigaku Utima IV X-ray diffract meter, which was equipped with Cu Kα radiation. The XRD data were collected at the range of 10 to 80° with 5°/min scan rate. The reducibility of the catalysts was measured by a Quantachrom automatic chemisorption analyzer to obtain the hydrogen temperature programmed reduction curve (H$_2$-TPR). 0.05 g catalyst was placed in a mixed gas stream of 10 vol.% H$_2$/Ar and then heated to 800 °C at the programmed temperature rate of 10 °C/min. The X-ray photoelectron spectroscopy (XPS) of the samples was measured using an X-ray photoelectron spectrometer equipped with an Al Kα excitation source, whose model number was Thermo ESCALAB 250Xi.

Results and Discussion

Catalytic oxidation of toluene, ethyl acetate and chlorobenzene. *Catalytic activity.* The results of the degradation evaluation in three VOCs oxidation including toluene, ethyl acetate and chlorobenzene are shown in Fig. 2(a–c). From these, it is easy to see that the conversion of VOCs rose with the increase of the reaction temperature, and R-Ag/MnO$_2$-cordierite showed better catalytic activity than T-Ag/MnO$_2$-cordierite. T$_{90}$ (Temperature corresponding to the VOCs conversion of 90%) is commonly used to evaluate and compare the catalytic activity of samples. With regard to the R-Ag/MnO$_2$-cordierite, the values of T$_{90}$ for ethyl acetate, toluene and chlorobenzene conversion were 217 °C, 275 °C and 385 °C, which were lower than those of T-Ag/MnO$_2$-cordierite (260 °C, 330 °C and 420 °C), indicating that the R-Ag/MnO$_2$-cordierite has better catalytic activity than T-Ag/MnO$_2$-cordierite. It is worth pointing out that, with the same conversion rate, the degradation temperature required for toluene and chlorobenzene displays higher than ethyl acetate. The reason may be related to the different strength between reactants and catalyst surface. It has been found that aromatic hydrocarbon compounds composed of one saturated chain and one benzene ring have a strong interaction with the surface of catalysts, making them easier to compete with oxygen for adsorption and occupy more active sites during the reaction[29]. What's more, comparing with other powder catalysts (MnO$_x$/γ-Al$_2$O$_3$[21], Pt/TiO$_2$[17] and nano-octahedra Ru/CeO$_2$[30]), R-Ag/MnO$_2$-cordierite molded catalyst prepared in this study requires much lower temperature for catalytic degradation of Cl-VOCs.

Catalysts stability. R-Ag/MnO$_2$-cordierite with high catalytic activity was selected to investigate the stability of the catalysts, shown in Fig. 3. It is easy to see that the conversion of ethyl acetate and toluene remained stable for 24 h (above 95%). For the conversion of chlorobenzene, it remained 90% within first 12 h and dropped slightly for the next 12 h, which still is located at above 85% within 24 hours. This result indicates that R-Ag/MnO$_2$-cordierite has great stability to VOCs and exhibits certain anti-toxicity performance to chlorobenzene. The physical properties of R-Ag/MnO$_2$-cordierite reacted with chlorobenzene for 24 h (denoted as R$_{CB}$-Ag/MnO$_2$) was carried out in section 3.2.

Effect of space velocity. In industrial applications, space velocity has been reported to be a critical factor affecting catalytic oxidation and devices economy. Effect of space velocity on catalytic activity of R-Ag/MnO$_2$-cordierite has been studied, which is shown in the Fig. 4. Obviously, the degradation effect of R-Ag/MnO$_2$-cordierite is reduced slightly with the increasing of space velocity from 10,000 h^{-1} to 40,000 h^{-1}, where the catalyst ignition
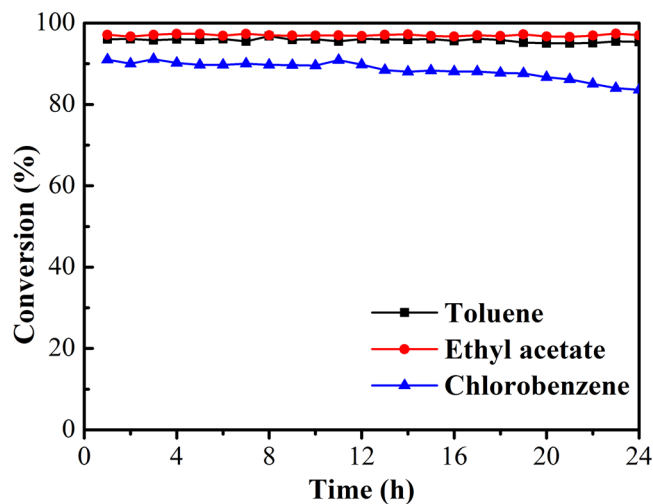
Figure 3. Stability tests of R-Ag/MnO$_2$-cordierite for toluene, ethyl acetate and chlorobenzene; reaction conditions: temperature = 280 °C for toluene, 230 °C for ethyl acetate, 390 °C for chlorobenzene; VOCs = 1000 ppm; catalyst content = 0.1 g/cm^3; SV = 10,000 h^{-1}.
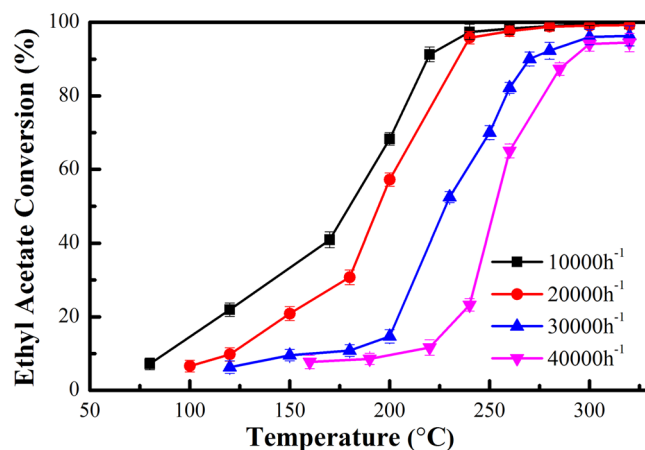

Figure 4. Catalytic removal efficiency of R-Ag/MnO$_2$-cordierite on ethyl acetate at different space velocity; reaction conditions: VOCs = 1000 ppm; catalyst content = 0.1 g/cm^3.

SV/h^{-1}	Ignition temperature/°C	T$_{90}$/°C
10,000	125	217
20,000	150	230
30,000	200	265
40,000	225	287

Table 1. Ignition temperature and T$_{90}$ of ethyl acetate oxidation with different space velocities.

temperature and T$_{90}$ of ethyl acetate have risen by approximately 100 °C and 70 °C respectively at a higher SV of 40,000 h^{-1} (still lower than 300 °C, Table 1). This result indicates that the catalyst have promise for adoption by the industry due to its high activity at high space velocity.

Physical properties of the catalysts. The elemental composition of the catalysts was measured by ICP-MS, and the results are shown in Table 2. The contents of Mn and Ag in the catalyst were about 42.6 wt% and 1.9 wt%, respectively. The Ag content coincides with the theoretical ratio of 2 wt% after deducting the aluminum sol component, which means that the noble metal Ag has been loaded into MnO$_2$ successfully.

Figure 5 is the XRD patterns of the three catalysts. The presence of aluminum sol on the oxide supports had no effect on crystal formation of the catalysts (shown in SI-2). It is found that all samples in the 2θ range of 10–80° exhibit characteristic diffraction peaks of α-MnO$_2$ (ICSD PDF 44–0141) and Ag (111) crystal plane at

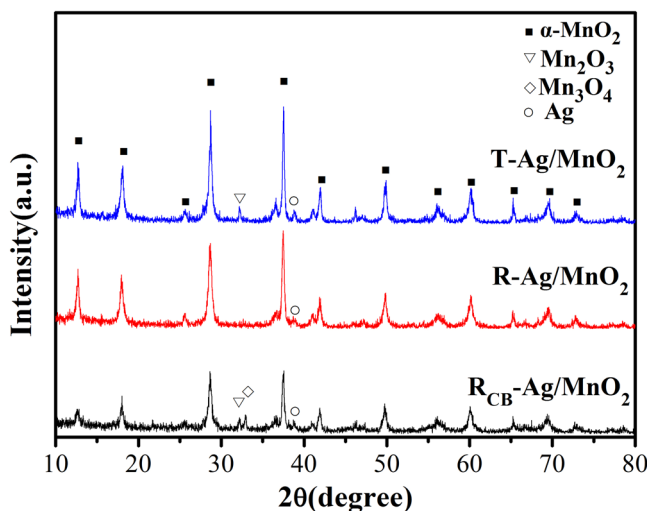| Samples	Mn/wt%	Ag/wt%	Al/wt%	Ag/wt% (Al deducted)
T-Ag/MnO$_2$	42.24	1.54	8.13	1.93
R-Ag/MnO$_2$	41.97	1.53	7.97	1.91
R$_{CB}$-Ag/MnO$_2$	42.66	1.51	8.51	1.89

Table 2. Catalysts element components.

Figure 5. XRD patterns of Ag/MnO$_2$ catalysts.

38.1° (PDF#65-2871)[15]. An additional diffraction peak of T-Ag/MnO$_2$ is observed at 32.5° assigning to Mn$_2$O$_3$ comparing with R-Ag/MnO$_2$, which was probably due to the addition of HCl during preparation. Furthermore, the diffraction peaks of Mn$_2$O$_3$ and Mn$_3$O$_4$ (32.5° and 33.0°[14]) appeared and the peak intensity of α-MnO$_2$ significantly weakened in the pattern of R$_{CB}$-Ag/MnO$_2$. This result was related with the structural transformation of α-MnO$_2$ to Mn$_2$O$_3$ and Mn$_3$O$_4$, which may take place in the process of catalytic degradation of chlorobenzene. Related studies[12] have shown that manganese oxides exhibit different activity in some benzenes catalytic oxidation reaction. Higher oxidation state of Mn species, namely MnO$_2$, is preferable for oxidation reactions over Mn$_2$O$_3$ and Mn$_3$O$_4$. Combined with results of 3.1.1, it is reasonable to suggest that the catalytic activity of R-Ag/MnO$_2$-cordierite with pure α-MnO$_2$ is superior to that of T-Ag/MnO$_2$-cordierite with mixed α-MnO$_2$ and Mn$_2$O$_3$. Moreover, it was assumed that the formation of lower manganese oxides was responsible of a decrease in activity of R-Ag/MnO$_2$-cordierite after chlorobenzene catalytic oxidation.

The SEM images of each sample are shown in the Fig. 6. Nanotube and nanorod morphology were observed in Fig. 6(b,d), and no clear differences in size or shape was detected in Fig. 6(a,b) or Fig. 6(c,d), indicating that the existence of aluminum sol has no influence in Ag/MnO$_2$ catalyst morphology. It was also found that there was little change between R-Ag/MnO$_2$ (Fig. 6(d)) and R$_{CB}$-Ag/MnO$_2$ (Fig. 6(f)), except that the nanorod length of R$_{CB}$-Ag/MnO$_2$ was shorter.

Figure 7 reveals TEM images of Ag/MnO$_2$ samples and SEM element mapping images of the R-Ag/MnO$_2$. The Ag loaded on the catalyst with good dispersion (about 5 nm) and the Ag/MnO$_2$ catalysts retained fine crystalline structure. The lattice spacing of the (110) and (111) crystal plane was 0.310 nm and 0.235 nm, respectively, which is in line with the corresponding values (0.310 nm) of standard α-MnO$_2$ sample (JCPDS PDF 72–1982) and (0.236 nm) of standard Ag sample (JCPDS PDF 04–0783). It has been observed that rod-like Ag/MnO$_2$ catalyst exhibits the higher VOCs conversion, whereas T-Ag/MnO$_2$ shows relatively low catalytic activity. This difference in catalytic activity is attributed to the catalyst morphology. To our knowledge, catalysts with different morphology can expose different active or specific energy crystal faces selectively and some of them with special morphology might promote the better dispersion of active components. That can be contributed greatly to improve catalytic reactivity, selectivity and stability[12]. For this study, the R-Ag/MnO$_2$ could be more favorable to increase the effective activated spot and improve the catalytic activity better than T-Ag/MnO$_2$. As reported, the degradation of chlorobenzene calls for higher requirements for the stability of catalysts[23]. The morphology of R-Ag/MnO$_2$ and the crystallinity of α-MnO$_2$ are no variation after degrading Cl-VOCs at high space velocity, indicating that R-Ag/MnO$_2$ catalyst has excellent mechanical strength and stability in this study.

H$_2$-TPR curves of Ag/MnO$_2$ catalysts are shown in Fig. 8. A large broad and strong peak at about 226 °C of the R-Ag/MnO$_2$ pattern could be considered as the transformation from high-valent manganese ions to lower valence state. For T-Ag/MnO$_2$ catalyst, the reduction peak and a shoulder peak shifted to the higher temperatures at 355 °C and 377 °C compared to R-Ag/MnO$_2$. This indicates that R-Ag/MnO$_2$ possesses better low temperature reduction performance than T-Ag/MnO$_2$. After catalytic oxidation of chlorobenzene, the main reduction peaks of Mn species for R$_{CB}$-Ag/MnO$_2$ are shifted to higher temperature and could be regarded as two peaks at about
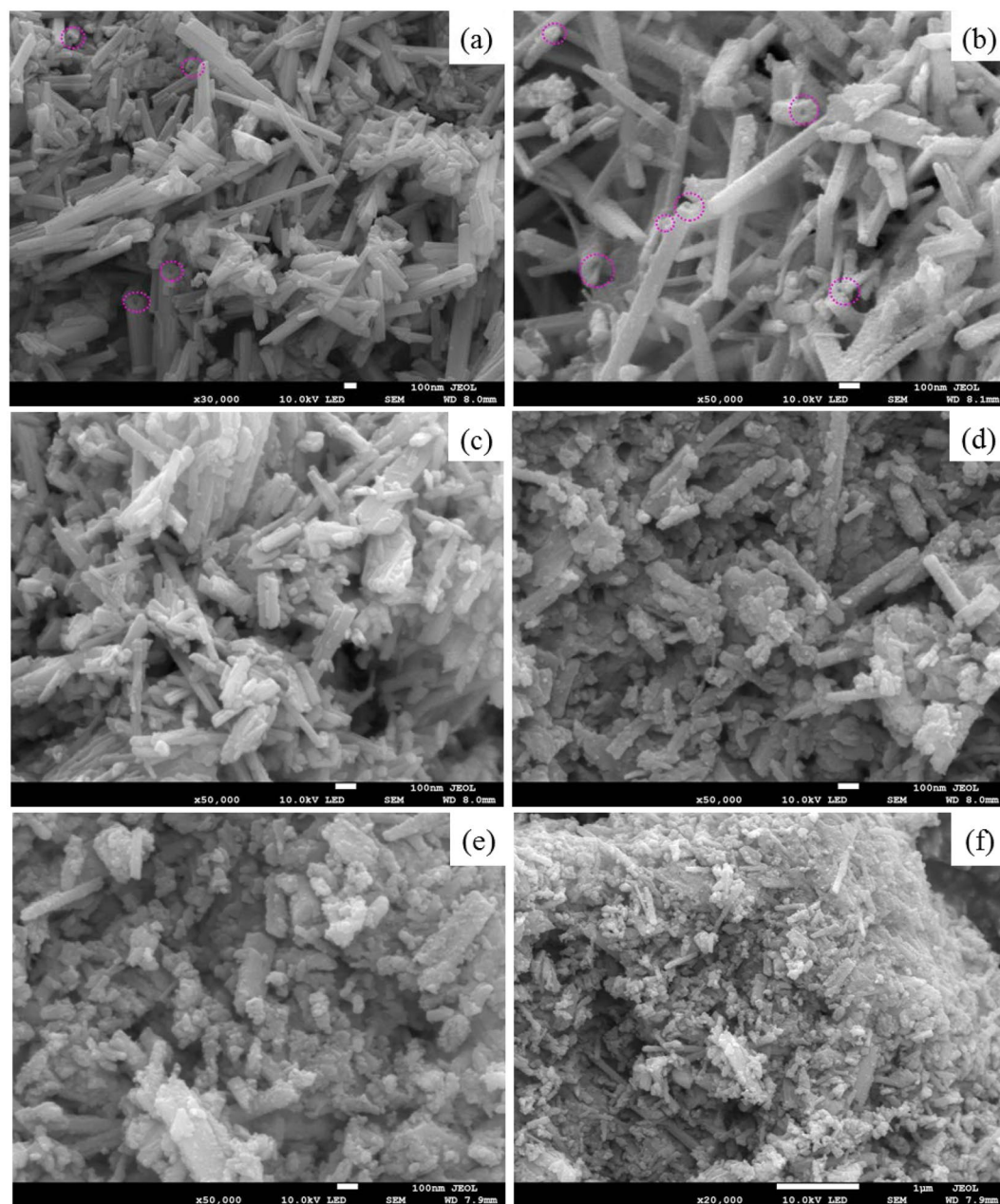
Figure 6. SEM image of (**a**) T-Ag/MnO$_2$, (**b**) T-Ag/MnO$_2$ with aluminum sol, (**c**) R-Ag/MnO$_2$, (**d**) R-Ag/MnO$_2$ with aluminum sol, (**e,f**) R$_{CB}$-Ag/MnO$_2$ with aluminum sol.

263 °C and 308 °C, which means the reduced reducibility may be one reason of the slight decrease in catalytic activity (combined with results of 3.1.2). In the light of previous results[12,31], the transformation process of MnO$_2$ can be reasonably interpreted as two steps: (1) MnO$_2$→Mn$_2$O$_3$ corresponding to peaks at 226 °C, 263 °C and 355 °C, (2) Mn$_2$O$_3$→Mn$_3$O$_4$ corresponding to peaks at 308 °C and 377 °C, respectively. As mentioned previously[13], the presence of more high-valence manganese is beneficial to the low-temperature catalytic oxidation of VOCs. Combined with the results of XRD, it can be inferred that R-Ag/MnO$_2$-cordierite with high valence state of manganese may be the reasons for the strong reducibility and higher catalytic activity[32].

Figure 9 illustrates the Mn 2p, O 1s, Ag 3d and Cl 2p XPS spectra of Ag/MnO$_2$ catalysts. The Mn 2p peaks appeared at 642.2 eV and 641.5 eV, which are attributed to the Mn^{4+} and Mn^{3+}, respectively[13,33,34]. Compared with R-Ag/MnO$_2$, the chemical valence of Mn of T-Ag/MnO$_2$ is mainly in Mn^{4+} oxidation state and a small quantity of Mn^{3+} co-existed. It has been verified that the higher extent of the Mn^{4+} favors the redox reactions and gives a boost to the catalytic performance of VOCs degradation[35], as well as the presence of element Mn plays a facilitating role in the production of oxygen vacancies and the enhancement of oxygen mobility[36]. From Table 3, it could be found that the molar ratio of surface Mn^{4+} of R-Ag/MnO$_2$ is higher comparing with T-Ag/MnO$_2$, which gives rise to the fact that the nanorod Ag/MnO$_2$ molded catalyst exhibited good catalytic activity for VOCs. In addition, Mn^{4+}/Mn value (0.75) of R$_{CB}$-Ag/MnO$_2$ was markedly reduced because of the reduction of MnO$_2$ to Mn$_2$O$_3$ during catalytic
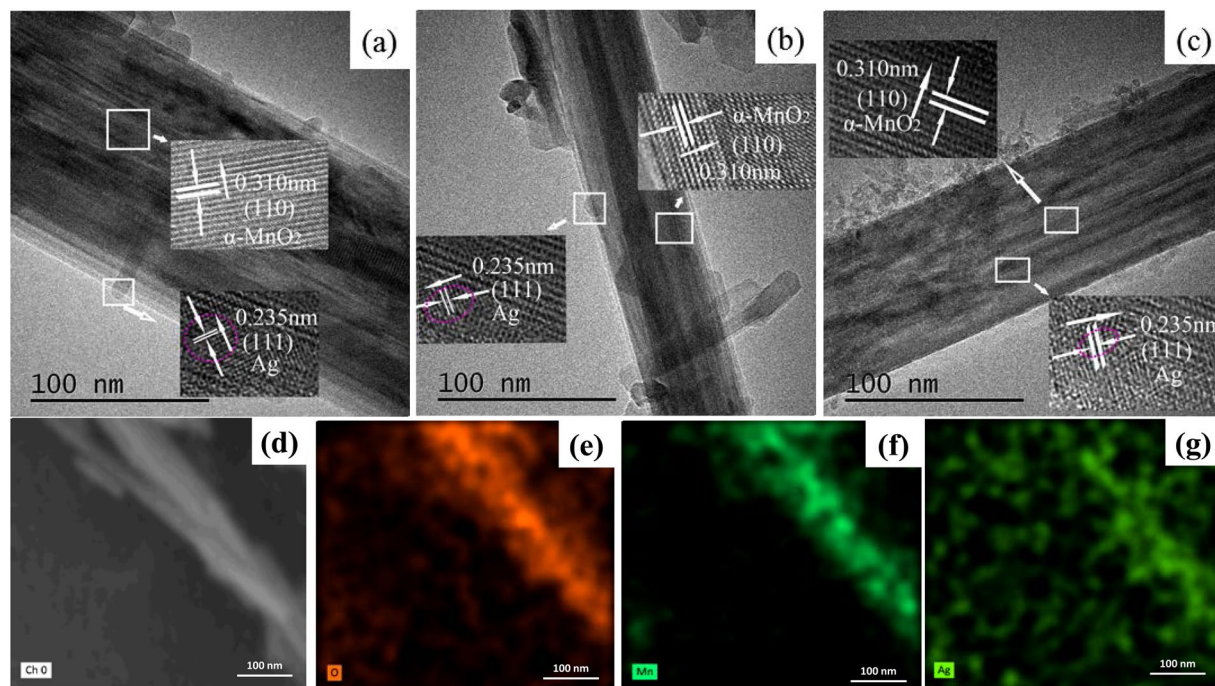
Figure 7. TEM micrograph of the (**a**) T-Ag/MnO$_2$, (**b**) R-Ag/MnO$_2$, (**c**) R$_{CB}$-Ag/MnO$_2$ with aluminum sol; (**d**–**g**) SEM element mapping images of the R-Ag/MnO$_2$.
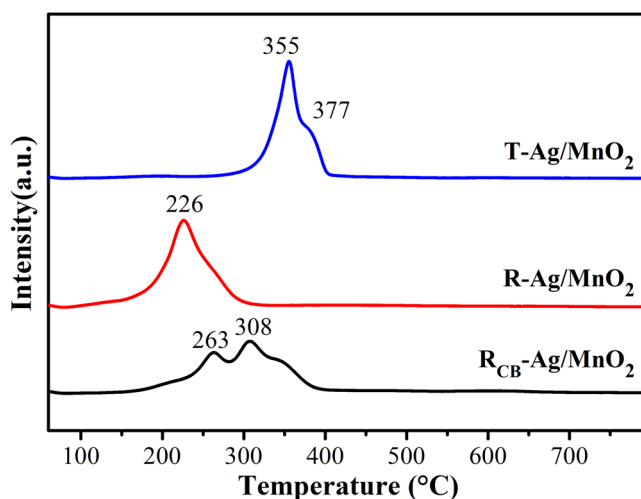

Figure 8. H$_2$-TPR profiles of Ag/MnO$_2$ catalysts.

oxidation of chlorobenzene. The results were also consistent with the aforementioned XRD and H$_2$-TPR. According to the XPS spectrum of O1s, the peak at 529.6 could be ascribed to the lattice oxygen (O$_{latt}$), while the peak at 531.7 eV could be ascribed to the adsorbed oxygen (O$_{ads}$)[14]. As reported[20,37], the atomic ratio of the O$_{latt}$/O$_{ads}$ could influence the catalytic oxidation of VOCs. Different oxygen species content in each catalyst was obtained according to XPS characterization (shown in the Table 3). The amount of O$_{latt}$/O$_{ads}$ of R-Ag/MnO$_2$ is much higher than that of T-Ag/MnO$_2$, suggesting that rod-like Ag/MnO$_2$ may be beneficial to the lattice oxygen migration, which should administer to enhance the performance of R-Ag/MnO$_2$ for the catalytic oxidation of VOCs. Besides, the O$_{latt}$/O$_{ads}$ value of R$_{CB}$-Ag/MnO$_2$ is significantly much less in comparison with that of R-Ag/MnO$_2$. The result can be attributed to the fact that lattice oxygen facilitates the VOCs oxidation reaction at low temperatures.

The peaks at 373.8 eV and 367.8 eV according to the XPS spectrum of Ag 3d are assigned to the 3d$_{5/2}$ and 3d$_{3/2}$ of Ag, respectively, while the other two peaks at 372.9 eV and 366.8 eV are attributed to silver 3d$_{3/2}$ and 3d$_{5/2}$ of AgCl[38–42]. Apparently, the intensity of Ag 3d peak of R-Ag/MnO$_2$ was significantly reduced after catalytic oxidation with chlorobenzene. Furthermore, the Cl 2p XPS spectrum of R$_{CB}$-Ag/MnO$_2$ catalyst reveals two peaks at 199.9 eV and 198.3 eV, which represent Cl 2p$_{3/2}$ and Cl 2p$_{1/2}$ binding energy separately[39–41]. According to the
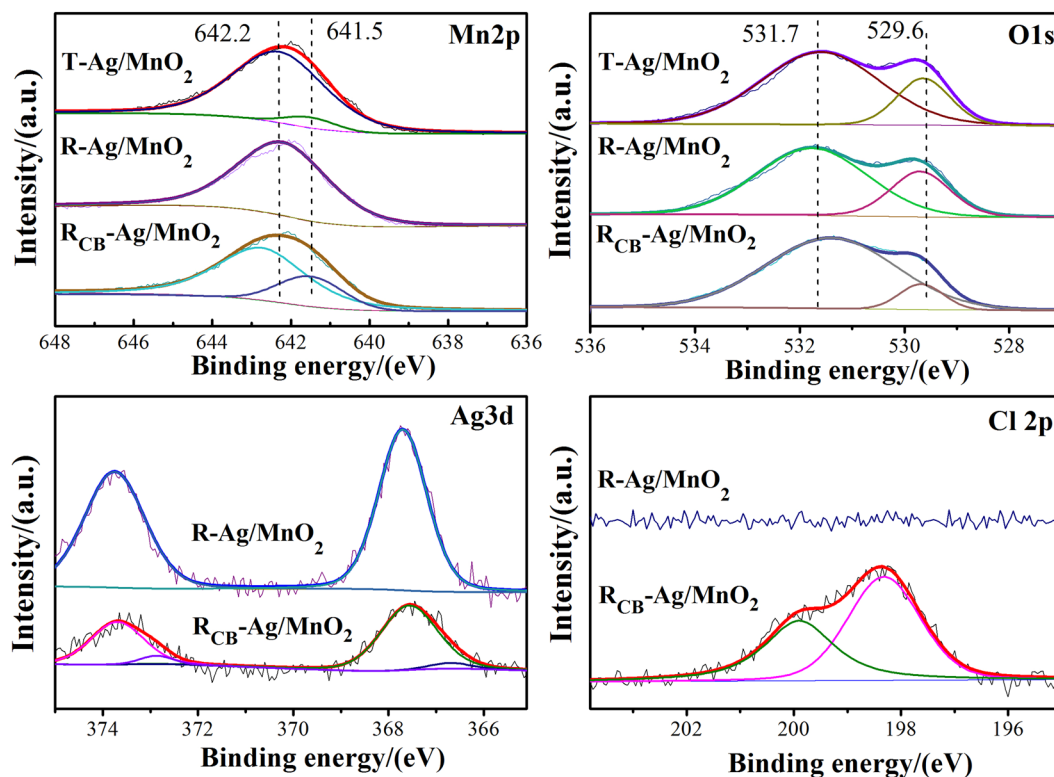
Figure 9. Mn 2p, O 1s, Ag 3d and Cl 2p XPS spectrum of Ag/MnO_2.

Sample	BE (eV)		O_{latt}/O_{ads}	Mn^{4+}/Mn
	Lattice oxygen	Absorbed oxygen		
$T-Ag/MnO_2$	529.6	531.6	0.47	0.93
$R-Ag/MnO_2$	529.7	531.7	0.61	1.00
$R_{CB}-Ag/MnO_2$	529.7	531.4	0.14	0.75

Table 3. Contents of different oxygen species and manganese.

results of stability test, it is speculated that small amounts of AgCl are formed and accumulated over the catalyst surface to inactive catalyst, which may be the reason for the slight decrease in activity of $R-Ag/MnO_2$-cordierite during the long-term reaction with chlorobenzene.

From all the characterization results, the $R-Ag/MnO_2$-cordierite molded catalyst shows higher activity to remove VOCs than $T-Ag/MnO_2$-cordierite molded catalyst due to several reasons. According to the XRD, H_2-TPR and XPS, it's easy to find that manganese with a high valence state could carry more lattice oxygen and possess stronger reducibility contributed to higher catalytic activity of the nanorod Ag/MnO_2. Besides, it also can be seen from the results of SEM and TEM that the rod-like morphology and fine crystalline structure of catalysts determine the excellent mechanical strength and stability, thus leading to the high catalytic stability at higher space velocity. Last but not least, the presence of silver could accelerate the lattice oxygen migration on MnO_2 during VOCs oxidation process, which should administer to enhance the performance of $R-Ag/MnO_2$ for the catalytic oxidation of VOCs.

Conclusions

In this study, Ag/MnO_2 with nanorod and nanotube morphology supported on honeycomb cordierite catalysts were successfully synthesized using a liquid phase reduction method. Various characterization techniques were used to investigate their physicochemical properties and the catalytic oxidation mechanism of toluene, ethyl acetate and chlorobenzene. The Ag/MnO_2-cordierite molded catalyst with nanorod morphology performs much better than other catalysts because of high valence manganese oxide, more active lattice oxygen content and preferred low-temperature reducibility. Experimental results show that the nanorod Ag/MnO_2-cordierite exhibits T_{90} for toluene, ethyl acetate and chlorobenzene conversion at 275 °C, 217 °C and 385 °C respectively under the space velocity of 10,000 h^{-1}. For the different space velocity and catalytic stability test, nanorod Ag/MnO_2-cordierite show best mechanical strength, better catalytic durability and satisfied anti-toxicity to chlorobenzene at higher space velocity. These results reveal that the molded catalyst is characterized by lower cost, higher activity and stability as well as anti-chlorine poisoning ability. It has industrial application prospects in the oxidation of different kinds of VOCs.

References

1. Zawadzki, M. & Okal, J. Effect of Co and Fe substitution on catalytic VOCs removal on zinc aluminate. *Catalysis Today* **257**, 136–143, https://doi.org/10.1016/j.cattod.2015.01.022 (2015).
2. Scirè, S. & Liotta, L. F. Supported gold catalysts for the total oxidation of volatile organic compounds. *Applied Catalysis B: Environmental* **125**, 222–246, https://doi.org/10.1016/j.apcatb.2012.05.047 (2012).
3. Joung, H.-J. *et al.* Catalytic oxidation of VOCs over CNT-supported platinum nanoparticles. *Applied Surface Science* **290**, 267–273, https://doi.org/10.1016/j.apsusc.2013.11.066 (2014).
4. Bedia, J., Rosas, J. M., Rodríguez-Mirasol, J. & Cordero, T. Pd supported on mesoporous activated carbons with high oxidation resistance as catalysts for toluene oxidation. *Applied Catalysis B: Environmental* **94**, 8–18, https://doi.org/10.1016/j.apcatb.2009.10.015 (2010).
5. Solsona, B. *et al.* Total oxidation of VOCs on mesoporous iron oxide catalysts: Soft chemistry route versus hard template method. *Chemical Engineering Journal* **290**, 273–281, https://doi.org/10.1016/j.cej.2015.12.109 (2016).
6. Tang, W. *et al.* Synergistic Effects in Porous Mn-Co Mixed Oxide Nanorods Enhance Catalytic Deep Oxidation of Benzene. *Catalysis Letters* **144**, 1900–1910, https://doi.org/10.1007/s10562-014-1340-3 (2014).
7. Zeng, J., Liu, X., Wang, J., Lv, H. & Zhu, T. Catalytic oxidation of benzene over MnO_x/TiO_2 catalysts and the mechanism study. *Journal of Molecular Catalysis A: Chemical* **408**, 221–227, https://doi.org/10.1016/j.molcata.2015.07.024 (2015).
8. Brunet, J. *et al.* Co-Al-Ce Mixed Oxide Materials Prepared by Hydrotalcite Way for VOCs Total Oxidation in Micro- and Semi-Pilot Scale. *Materials Today: Proceedings* **3**, 188–193, https://doi.org/10.1016/j.matpr.2016.01.055 (2016).
9. Aguero, F. N., Scian, A., Barbero, B. P. & Cadús, L. E. Combustion of volatile organic compounds over supported manganese oxide: Influence of the support, the precursor and the manganese loading. *Catalysis Today* **133-135**, 493–501, https://doi.org/10.1016/j.cattod.2007.11.044 (2008).
10. Si, W., Wang, Y., Zhao, S., Hu, F. & Li, J. A Facile Method for *in Situ* Preparation of the $MnO_2/LaMnO_3$ Catalyst for the Removal of Toluene. *Environ Sci Technol* **50**, 4572–4578, https://doi.org/10.1021/acs.est.5b06255 (2016).
11. Kim, S. C. & Shim, W. G. Catalytic combustion of VOCs over a series of manganese oxide catalysts. *Applied. Catalysis B: Environmental* **98**, 180–185, https://doi.org/10.1016/j.apcatb.2010.05.027 (2010).
12. Wang, F. *et al.* Manganese oxides with rod-, wire-, tube-, and flower-like morphologies: highly effective catalysts for the removal of toluene. *Environ Sci Technol* **46**, 4034–4041, https://doi.org/10.1021/es204038j (2012).
13. Si, W. *et al.* A high-efficiency gamma-MnO_2-like catalyst in toluene combustion. *Chemical communications* **51**, 14977–14980, https://doi.org/10.1039/c5cc04528b (2015).
14. Tang, X. *et al.* Complete oxidation of formaldehyde over Ag/MnO_x-CeO_2 catalysts. *Chemical Engineering Journal* **118**, 119–125, https://doi.org/10.1016/j.cej.2006.02.002 (2006).
15. Xie, S. *et al.* Excellent catalytic performance, thermal stability, and water resistance of 3DOM Mn_2O_3-supported Au-Pd alloy nanoparticles for the complete oxidation of toluene. *Applied Catalysis A: General* **507**, 82–90, https://doi.org/10.1016/j.apcata.2015.09.026 (2015).
16. Xie, S. *et al.* Effect of transition metal doping on the catalytic performance of Au-Pd/3DOM Mn_2O_3 for the oxidation of methane and o -xylene. *Applied Catalysis B: Environmental* **206**, 221–232, https://doi.org/10.1016/j.apcatb.2017.01.030 (2017).
17. Cao, S. *et al.* Bimodal mesoporous TiO_2 supported Pt, Pd and Ru catalysts and their catalytic performance and deactivation mechanism for catalytic combustion of Dichloromethane (CH_2Cl_2). *Applied Catalysis A: General* **550**, 20–27, https://doi.org/10.1016/j.apcata.2017.10.006 (2018).
18. Xia, Y. *et al.* Concurrent catalytic removal of typical volatile organic compound mixtures over Au-Pd/alpha-MnO_2 nanotubes. *J Environ Sci (China)* **64**, 276–288, https://doi.org/10.1016/j.jes.2017.06.025 (2018).
19. Yi, H. *et al.* Novel synthesis of Pd-$CeMnO_3$ perovskite based on unique ultrasonic intervention from combination of Sol-Gel and impregnation method for low temperature efficient oxidation of benzene vapour. *Ultrasonics Sonochemistry* **48**, 418–423, https://doi.org/10.1016/j.ultsonch.2018.06.009 (2018).
20. Li, J., Qu, Z., Qin, Y. & Wang, H. Effect of MnO_2 morphology on the catalytic oxidation of toluene over Ag/MnO_2 catalysts. *Applied Surface Science* **385**, 234–240, https://doi.org/10.1016/j.apsusc.2016.05.114 (2016).
21. Yang, P., Xue, X., Meng, Z. & Zhou, R. Enhanced catalytic activity and stability of Ce doping on Cr supported HZSM-5 catalysts for deep oxidation of chlorinated volatile organic compounds. *Chemical Engineering Journal* **234**, 203–210, https://doi.org/10.1016/j.cej.2013.08.107 (2013).
22. Liu, X., Chen, L., Zhu, T. & Ning, R. Catalytic oxidation of chlorobenzene over noble metals (Pd, Pt, Ru, Rh) and the distributions of polychlorinated by-products. *Journal of hazardous materials* **363**, 90–98, https://doi.org/10.1016/j.jhazmat.2018.09.074 (2018).
23. Huang, B., Lei, C., Wei, C. & Zeng, G. Chlorinated volatile organic compounds (Cl-VOCs) in environment - sources, potential human health impacts, and current remediation technologies. *Environment international* **71**, 118–138, https://doi.org/10.1016/j.envint.2014.06.013 (2014).
24. Xiao, B. *et al.* A green and facile synthesis of Co_3O_4 monolithic catalyst with enhanced total oxidation of propane performance. *Catalysis Communications* **116**, 1–4, https://doi.org/10.1016/j.catcom.2018.07.013 (2018).
25. Zhou, T., Li, L., Cheng, J. & Hao, Z. Preparation of binary washcoat deposited on cordierite substrate for catalytic applications. *Ceramics International* **36**, 529–534, https://doi.org/10.1016/j.ceramint.2009.09.027 (2010).
26. Ma, W. J. *et al.* Catalytic combustion of toluene over Fe-Mn mixed oxides supported on cordierite. *Ceramics International* **39**, 277–281, https://doi.org/10.1016/j.ceramint.2012.06.022 (2013).
27. Kan, J. *et al.* Performance of co-doped Mn-Ce catalysts supported on cordierite for low concentration chlorobenzene oxidation. *Applied Catalysis A-General* **530**, 21–29, https://doi.org/10.1016/j.apcata.2016.11.013 (2016).
28. Zhang, W., Tang, A. & Xue, J. Preparation of Cr-MnO_x/Cordierite and Their Properties for Catalytic Oxidation of 1, 2-Dichlorobenzene. *Spectroscopy and Spectral Analysis* **36**, 3075–3082 (2016).
29. He, C., Li, P., Cheng, J., Hao, Z.-P. & Xu, Z.-P. A Comprehensive Study of Deep Catalytic Oxidation of Benzene, Toluene, Ethyl Acetate, and their Mixtures over Pd/ZSM-5 Catalyst: Mutual Effects and Kinetics. *Water, Air, & Soil Pollution* **209**, 365–376, https://doi.org/10.1007/s11270-009-0205-7 (2009).
30. Hsu, S.-H., Huang, C.-S., Chung, T.-W. & Gao, S. Adsorption of chlorinated volatile organic compounds using activated carbon made from Jatropha curcas seeds. *Journal of the Taiwan Institute of Chemical Engineers* **45**, 2526–2530, https://doi.org/10.1016/j.jtice.2014.05.028 (2014).
31. Qu, Z., Fan, R., Wang, Z., Wang, H. & Miao, L. Selective catalytic oxidation of ammonia to nitrogen over MnO_2 prepared by urea-assisted hydrothermal method. *Applied Surface Science* **351**, 573–579, https://doi.org/10.1016/j.apsusc.2015.05.154 (2015).
32. Xu, R., Wang, X., Wang, D., Zhou, K. & Li, Y. Surface structure effects in nanocrystal MnO_2 and Ag/MnO_2 catalytic oxidation of CO. *Journal of Catalysis* **237**, 426–430, https://doi.org/10.1016/j.jcat.2005.10.026 (2006).
33. Piumetti, M., Fino, D. & Russo, N. Mesoporous manganese oxides prepared by solution combustion synthesis as catalysts for the total oxidation of VOCs. *Applied Catalysis B: Environmental* **163**, 277–287, https://doi.org/10.1016/j.apcatb.2014.08.012 (2015).
34. Garcia, T. *et al.* Total oxidation of naphthalene using bulk manganese oxide catalysts. *Applied Catalysis A: General* **450**, 169–177, https://doi.org/10.1016/j.apcata.2012.10.029 (2013).
35. Bin, H. C., Pan, K. L. & Chang, M. B. Catalytic oxidation of trichloroethylene from gas streams by perovskite-type catalysts. *Environmental Science and Pollution Research* **25**, 11584–11594, https://doi.org/10.1007/s11356-018-1440-5 (2018).

36. Xing, X. *et al.* Synthesis of mixed Mn-Ce-O-x one dimensional nanostructures and their catalytic activity for CO oxidation. *Ceramics International* **41**, 4675–4682, https://doi.org/10.1016/j.ceramint.2014.12.014 (2015).

37. Farhang, Y., Taheri-Nassaj, E. & Rezaei, M. Pd doped LaSrCuO$_4$ perovskite nano-catalysts synthesized by a novel solid state method for CO oxidation and Methane combustion. *Ceramics International* **44**, 21499–21506, https://doi.org/10.1016/j.ceramint.2018.08.211 (2018).

38. Dong, R. *et al.* Ecofriendly Synthesis and Photocatalytic Activity of Uniform Cubic Ag@AgCl Plasmonic Photocatalyst. *J. Phys. Chem. C* **117**, 213–220, https://doi.org/10.1021/jp311970k (2013).

39. Dong, L., Liang, D. & Gong, R. *In Situ* Photoactivated AgCl/Ag Nanocomposites with Enhanced Visible Light Photocatalytic and Antibacterial Activity. *Eur. J. Inorg. Chem.*, 3200–3208, https://doi.org/10.1002/ejic.201200172 (2012).

40. Ai, L., Zhang, C. & Jiang, J. Hierarchical porous AgCl@Ag hollow architectures: Self-templating synthesis and highly enhanced visible light photocatalytic activity. *Applied. Catalysis B: Environmental* **142**, 744–751, https://doi.org/10.1016/j.apcatb.2013.05.053 (2013).

41. Sun, L., Zhang, R., Wang, Y. & Chen, W. Plasmonic Ag@AgCl Nanotubes Fabricated from Copper Nanowires as High-Performance Visible Light Photocatalyst. *ACS Applied Materials & Interfaces* **6**, 14819–14826, https://doi.org/10.1021/am503345p (2014).

42. Sun, H. *et al.* Effective and regenerable Ag/4A zeolite nanocomposite for Hg^0 removal from natural gas. *Journal of Alloys and Compounds* **762**, 520–527, https://doi.org/10.1016/j.jallcom.2018.05.222 (2018).

Acknowledgements

Author Contributions

Experiment and article were finished by Jianan Zhu, and instructed by Professor Peng Liang and Wenrui Zhang. Dr. Yaqing Zhang, M.S. Qiuping Qi, Professor Huawei Zhang and Dekui Sun also offer their guidance and comments for our experiments. All authors had reviewed and given approval to the final version of the manuscript.

Additional Information

Supplementary information accompanies this paper at https://doi.org/10.1038/s41598-019-48506-5.

Competing Interests: The authors declare no competing interests.

Publisher's note: Springer Nature remains neutral with regard to jurisdictional claims in published maps and institutional affiliations.